NanoMAX: A hard x-ray nanoprobe beamline at MAX IV

Ulf Johansson*[a], Ulrich Vogt[b], Anders Mikkelsen[c]
[a]MAX IV Laboratory, Lund University, Box 118, 221 00 Lund, Sweden
[b]Biomedical and X-Ray Physics, Department of Applied Physics, KTH/Royal Institute of Technology, Albanova University Center, 106 91 Stockholm, Sweden
[c]Synchrotron Radiation Research, Department of Physics, Lund University, Box 118, 221 00 Lund, Sweden

ABSTRACT

We describe the design of the NanoMAX beamline to be built among the first phase beamlines of the MAX IV facility in Lund, Sweden. NanoMAX will be a hard X-ray imaging beamline providing down to 10 nm in direct spatial resolution, enabling investigations of very small heterogeneous samples exploring methods of diffraction, scattering, absorption, phase contrast and fluorescence. The beamline will have two experimental stations using Fresnel zone plates and Kirkpatrick-Baez mirror optics for beam focusing, respectively. This paper focuses on the optical design of the beamline excluding the experimental stations but also describes general ideas about the endstations and the nano-focusing optics to be used. The NanoMAX beamline is planned to be operational late 2016.

Keywords: X-ray imaging, X-ray microscopy, X-ray optics, Nanoprobe, Synchrotron radiation, Ray tracing, MAX IV

1. INTRODUCTION

The new Swedish synchrotron radiation facility MAX IV is currently under construction in Lund in the south of Sweden. It will consist of a linear accelerator for full energy, top-up injections and two storage rings, one with 1.5 GeV and one with 3.0 GeV electron energy. The linear accelerator will also serve as the electron source for a short pulse facility and, in a possible future upgrade, a free electron laser. Eight initial beamlines have been funded and are planned to be operational in 2016.

The NanoMAX beamline will be built at the 3 GeV storage ring, an ultra-low emittance ring ideally suited for this type of beamline. It is a hard X-ray imaging beamline for micro- and nano-beams and will enable imaging applications exploring absorption, diffraction, scattering, and fluorescence methods. This type of beamline opens up for new opportunities within a very broad range of research fields[1], with the possibility to study nanoscale objects with atomic scale precision in realistic environments and in complex heterogeneous structures. As a result, one or more hard X-ray micro/nano imaging beamlines[2-5] either have been constructed or are under construction at virtually all synchrotrons with sufficiently high brightness. In the design phase of the present beamline several of these other designs have been carefully studied.

The NanoMAX beamline will feature two experimental stations. The first station will use zone plates to reach smallest focus sizes with the long term goal to achieve a direct 10 nm spatial resolution. The second station will use Kirkpatrick-Baez mirror optics with spot sizes down to 300 nm or better. The major components and characteristics of the beamline are depicted in figure 1 and table 1. Experimental features of the beamline will be implemented in a sequential fashion, to allow a high quality in available methods. The beamline commissioning will start early 2016 and first user experiments are expected to be possible late 2016.

X-Ray Nanoimaging: Instruments and Methods, edited by Barry Lai, Proc. of SPIE Vol. 8851, 88510L

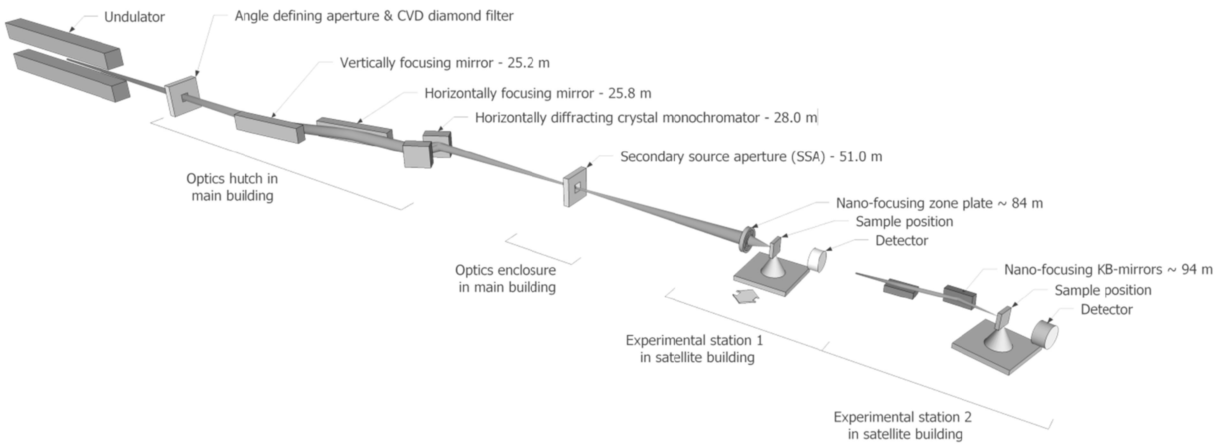

Figure 1. Major components of the NanoMAX beamline with two experimental stations.

Table 1. Main characteristics of the NanoMAX beamline.

Energy range	5 – 30 keV (3rd – 17th harmonic from undulator)
Photon source	In-vacuum undulator, 1.5 meter magnetic length, full harmonic overlap.
Beamline optics	Two horizontally deflecting mirrors focus the photon beam vertically and horizontally to form a secondary source, imaged by the nano-focusing optics.
Monochromator	Cryogenically cooled double crystal monochromator in horizontal diffraction geometry. Si(111) crystals.
Experimental station 1	Focusing with Fresnel zone plates. Spatial resolution 30 – 50 nm, final goal 10 nm. Sample scanning in X, Y and rotation.
Experimental station 2	Focusing with Kirkpatrick-Baez mirror system. Spatial resolution < 300 nm – 1 µm. Sample scanning in X, Y and rotation.
Main experimental methods	Scanning transmission X-ray microscopy (STXM), using absorption and phase contrast X-ray diffraction (XRD), X-ray fluorescence (XRF), Coherent diffraction imaging (CDI)

In this paper we first present the present stage of the design of the beamline and then we present the detailed optics simulations and considerations up to the experimental stations.

2. BEAMLINE DESIGN

2.1. Beamline overall outline and infrastructure

NanoMAX is approximately 100 meter long, extending into a satellite building adjacent to the main ring building. Figure 2 shows a drawing of the rooms and hutches for the beamline. The satellite building has a preparation room and a chemistry laboratory to support users in sample preparations. The beamline has a 20 m long experimental hutch, two control rooms, one for each experimental station and some office spaces.

Important for reliable operation of a beamline with the rather extreme spatial resolution goal of 10 nm are stable conditions in optics and experimental hutches. The ground underneath the 600 mm thick concrete floor of the main and satellite building is reinforced by mixing in concrete in the soil to approximately 4 meters depth. This is a very cost efficient way of achieving very low vibration levels with the geological conditions present at the MAX IV site. Temperature stability is also very important to minimize fluctuations within hours and days. The temperature in the experimental hutch is controlled to ± 0.1 K and special care is taken to reduce heat sources and heat dissipation to air. The hutch is constructed in concrete and built as a “hutch in a house” to passively aid temperature stability. An airlock helps in maintaining a stable temperature and clean conditions when persons have to enter the experimental hutch.

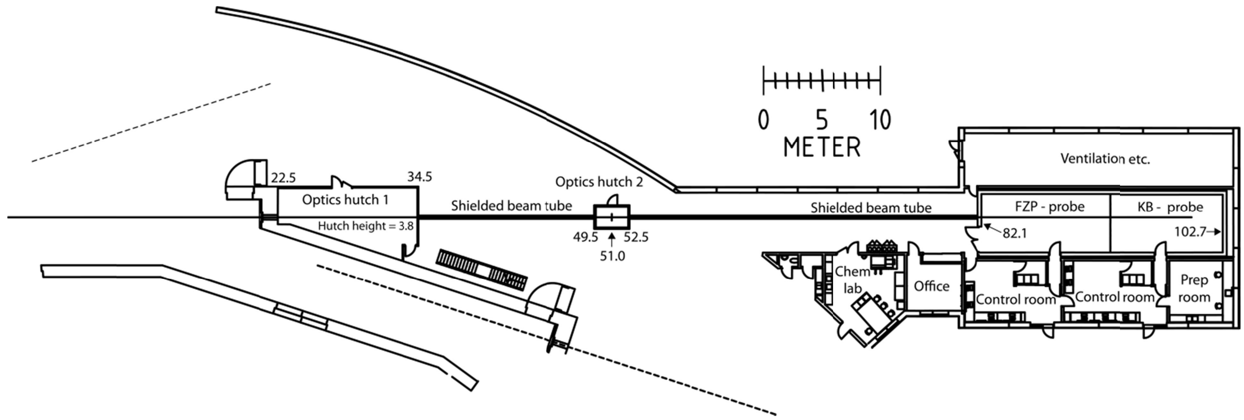

Figure 2. Floor plan for the NanoMAX beamline located in sector 3 of the MAX IV 3 GeV storage ring. Distances from the undulator, along the beamline, are indicated in the drawing.

2.2. Insertion device

The beamline will have an in-vacuum undulator with permanent magnets supplied by a commercial vendor. The period length is 18 mm, K_{MAX} is 1.92, minimum gap is 4.0 mm and total magnetic length is 1.5 m. The total power is 5.9 kW. The length of the present undulator may possibly be expanded to 2.0 m, while the straight section of the ring in-line with NanoMAX can hold a future undulator construction at a length of up to 3.7 m. The present design will give superior performance due to the specifications of the MAX IV ring, while still being a proven, reliable undulator technology. Figure 3 shows a calculated photon flux spectrum[6-7] to be expected from the 1.5 meter long undulator.

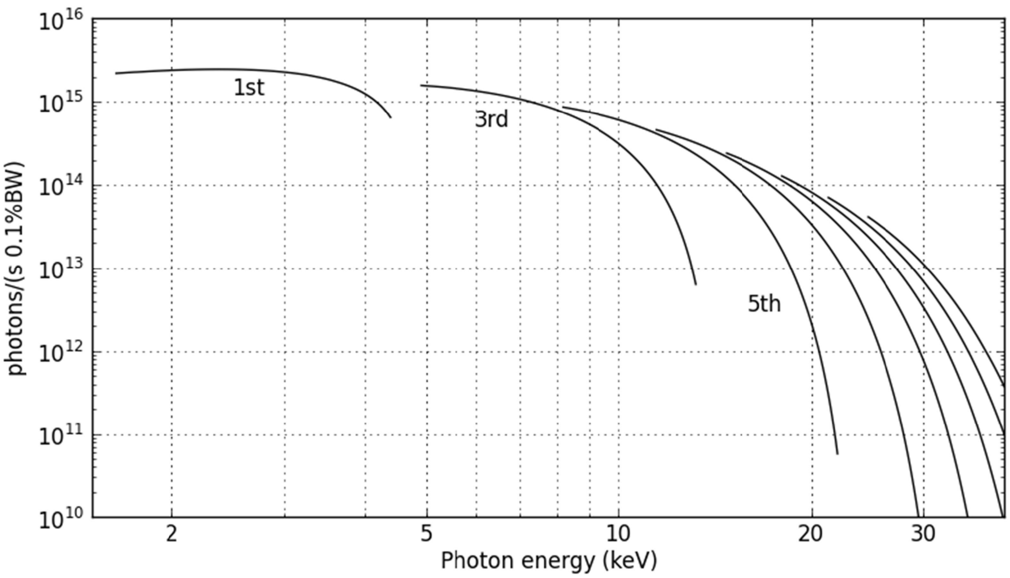

Figure 3. Photon flux from the undulator within 40x40 μrad^2 acceptance angle. Note: the first undulator harmonic will not be used by the beamline. The spectrum was calculated with the software code SPECTRA[6-7].

2.2. Front end & white beam filter

White beam masks in the front end absorb a majority of the power load from the undulator and reduce the photon beam acceptance angle. Movable slits in the front end are used to optimize the photon beam acceptance angle to the used nano-focusing optics and to reduce power load induced slope errors on the white beam optics. After final collimation in the optics hutch the maximum allowed acceptance angle is 40(H) x 40(V) μrad^2 corresponding to a maximum power load of about 100 W incident on the first focusing mirror. The beamline uses the 3rd harmonic and higher harmonics corresponding to a photon energy range of 5 – 30 keV. The first harmonic is attenuated with diamond CVD filters in front of the mirrors to reduce power load and power density on the mirrors and the monochromator crystals. It is possible to select filters with different thicknesses or run without filter.

A common design for the front end is used for all beamlines at the 3 GeV ring. In addition to fixed masks and movable slits for power load reduction the front end includes safety shutters, beam diagnostics, bremsstrahlung collimation and an electron beam deflector.

2.3. Beamline mirrors

The basic principle for the beamline optical design is the following. The undulator source is imaged into an intermediate point at 51 meter distance and simultaneously monochromated. This secondary source is in turn imaged by the nano-focusing optics; the KB-mirrors or the Fresnel zone plate.

Two white beam mirrors are used to focus the source into a stigmatic image at 51 meter distance from the undulator, where the secondary source aperture (SSA) is located. The first mirror (VFM) deflects the photon beam horizontally and focuses the beam in vertical direction by sagittal focusing. The second mirror (HFM) also deflects the beam horizontally and focuses the beam in horizontal direction by meridional focusing. The VFM has a fixed curvature while the HFM is bendable with cylindrical shape. The HFM has three coating stripes, Si, Rh and Pt. With the Si coating high harmonic contribution is reduced at photon energies below 10 keV. Rh is used in the range 10 – 22 keV and Pt above 22 keV. The VFM has a Pt coating. Both mirrors are water cooled with clamping to the mirror sides or by interfacing with eutectic metal. The most important mirror parameters are listed in table 2.

The geometry of deflecting the beam horizontally by both mirrors has some important advantages; the beam path is horizontal for the whole beamline; gravity does not act in the mirror meridional direction; slope errors influence the beam less in sagittal direction than in meridional direction. The latter is important because the undulator source size in vertical direction is only a few µm (FWHM). In horizontal direction the source size is about 100 µm, hence slope errors and vibrations in meridional direction are less apparent.

Table 2. Specifications for the vertically and horizontally focusing mirrors.

Mirror	**VFM**	**HFM**
Mirror substrate	Silicon	Silicon
Mirror shape	Circular cylinder (sagittal)	Circular cylinder (meridional)
Grazing angle of incidence	2.7 mrad	2.7 mrad
Optically active length	400 mm	400 mm
Coating stripe	Pt	Si, Rh, and Pt
Meridional slope error	< 0.5 µrad rms	< 0.5 µrad rms
Sagittal slope error	< 5 µrad rms	< 5 µrad rms
Micro roughness	<0.2 nm rms	<0.2 nm rms
Radius	68.84 mm (sagittal), fixed shape	9443 meter (meridional), bendable shape
Distance from source	25.2 m	25.8 m
Distance to image plane	25.8 m	25.2 m

2.4. Monochromator

A Si(111), cryo-cooled, fixed-beam, double-crystal monochromator (DCM) in horizontal diffraction geometry is following directly after the mirrors. We have chosen the horizontally deflecting design because we believe it improves beam stability. With this design small horizontal crystal vibrations do not significantly broaden the image of the source. Also the mechanical design can be made rigid and gravitational forces do not act in the diffraction direction. Drawbacks of the horizontal design are lower transmission in the 5 – 7 keV range and slightly worse energy resolution compared to a design with vertical diffraction geometry. However, with the relatively small size of the undulator source these drawbacks are less apparent. The most important parameters for the monochromator are listed in table 3.

Table 3. Most important parameters for the double crystal monochromator.

Crystals	Silicon (111)
Direction of diffraction	Horizontal, left on first crystal, right on second crystal, seen from above
Operation	Fixed beam offset, approximately 10 mm
Energy range	5-30 keV
Bragg angle range	23.3 – 3.7 °
Source distance	28 meter
Max. absorbed power	35 W
Max. absorbed power density	12 W / mm^2 (at 5 keV)

The monochromator and the two mirrors are situated in the first optical hutch. Space is also reserved in this hutch for a possible future upgrade with a double multilayer monochromator (DMM). With a DMM the photon flux can be increased one to two orders of magnitude which can be advantageous for, e.g., X-ray fluorescence measurements on low-concentration samples.

2.5. Secondary source aperture

The secondary source aperture (SSA) acts as a flexible source for the succeeding nano-focusing optics. The SSA consists of two pairs of slits, positioned 51 meters from the undulator source, where the vertical and horizontal opening can be set independently. By having this flexibility in defining the shape and size of the source the transverse coherence length can be tailored to match the Fresnel zone plates, KB-optics or other possible future optics, in order to reach spot sizes set by the diffraction limit. By opening the slits one can optimize for high flux conditions using enlarged spot sizes. The SSA is situated in a small temperature controlled optics hutch on the main ring floor. Together with the SSA a beam viewer and an X-ray beam position monitor (XBPM) is installed. The XBPM can be used to stabilize the beam position by regulating the pitch angle of the second crystal in the monochromator in a closed loop control.

2.6. Experimental stations

NanoMAX has two experimental stations and scanning X-ray microscopy is the fundamental imaging mode. Both stations are located in a 20 meter long experimental hutch in the satellite building. The hutch may possibly be divided by a radiation wall to allow for measuring with the first station while preparation work is done in the second half. Alternatively, by not dividing the hutch a third experimental setup may be possible to build if future ideas arise. The design of the two experimental stations is in an early phase. We have arranged two workshops to collect requests from potential future users and from international experts on nano-probe beamlines. At this time we have the following conceptual ideas.

The first experimental station, at approximately 33 meter distance from the SSA, uses Fresnel zone plates to achieve smallest possible focal spots. The realistic initial goal is to achieve a 30-50 nm spot within the energy range 5 – 12 keV. Zone plates will be developed and provided by a group from the Royal Institute of Technology in Stockholm. The long term goal is to achieve 10 nm spot size. Samples are scanned in X, Y for 2D mapping and also rotated for 3D mapping. Sample environments on this station have to be small because the available distance between optics and sample is in the mm to cm range and varies with photon energy. Thus for example in-situ sample environments have to be constructed in rather small dimensions. Such technologies have been successfully developed for a number of very different situations ranging from liquid cells[8] for biology to heated gas cells for catalysis[9].

The second experimental station, at approximately 43 meter distance from the SSA, uses two plane-elliptical mirrors in Kirkpatrick-Baez configuration to achieve a spot size in the 100 – 1000 nm range. Compared to the first station, the distance between optics and sample is more generous allowing for more complex and large sample setups. We expect this station to be configured with users' equipment rather frequently while for the FZP-station the setup will be more static and with a tighter integration between sample stage/environment and optics.

Main experimental methods are nano-diffraction, X-ray absorption, X-ray phase-contrast, X-ray fluorescence. We also plan to explore coherent diffraction imaging (CDI) methods, e.g., ptychography in various forms.

3. OPTICS SIMULATIONS

Ray tracing and heat load simulations have been done with the software package MASH[10] (Macros for Automation of SHadow) which integrates and automates the use of Shadow[11] for ray tracing and COMSOL multiphysics[12] for finite element analysis (FEA). MASH is very powerful in simulating beamline performance taking into account heat load induced distortions. In the simulations presented below we have used parameters very close to, but not identical, to the ones presented for the beamline under section 2.

3.1. Heat load management

The two mirrors VFM and HFM together with the first crystal of the monochromator are the components that can get distorted by power load. By carefully setting the angle defining aperture in the front end and by using the CVD diamond filter the incident power on the following optics is reduced. In the case of the two mirrors the FEA analysis shows that the temperature induced slope errors are smaller than the specified slope errors for the mirror manufacturing process. The power absorbed by the mirrors is only a few watts and handled by side cooling with water. In the thermal simulations the mirrors are cooled on both long sides at room temperature. A heat transfer coefficient of 0.3 W/(Kcm^2) was used.

The first monochromator crystal is absorbing most of the power and is also subject to the highest power density. The largest distortions occur at 5 keV where the Bragg angle is at maximum, 23.3º. Figure 4 shows this case where the maximum temperature on the crystal is 84 K and the power density is approximately 12 W/mm^2. For higher photon energies the Bragg angle decreases resulting in a larger illuminated footprint corresponding to reduced power density and crystal temperature. Above 10 keV the total power on the crystal is higher than at 5 keV because we use the Rh or Pt coating on the HFM but the power density is still below the case at 5 keV. In the thermal simulations the crystal is cooled on both long sides to the liquid nitrogen temperature of 77 K. A heat transfer coefficient of 0.3 W/(Kcm^2) was used. Water cooling temperatures were tested and found not feasible.

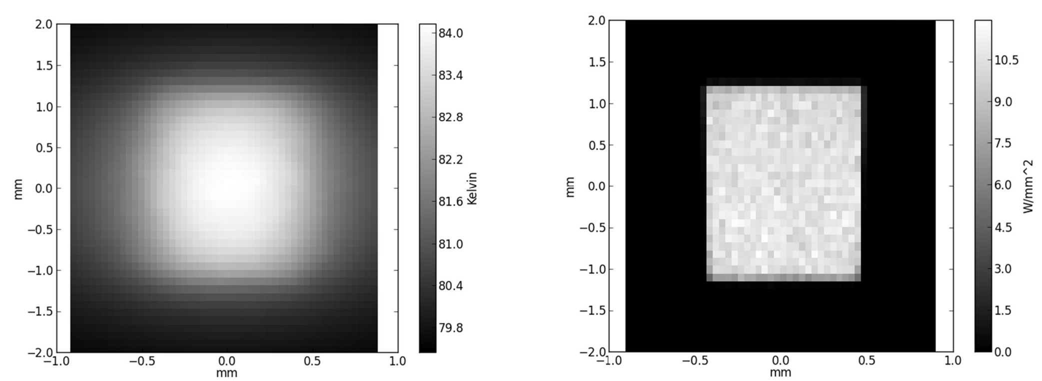

Figure 4. Temperature (left) and power density (right) on the first monochromator crystal at 5000 eV. Photon beam direction is upwards.

The temperature induced slope errors on the crystal are shown in figure 5. The maximum slope errors, peak-to-peak, are 3.2 µrad both in the meridional and sagittal directions, and occur at 5 keV. It should be noted that most of the useful beam intensity is centered on the crystal and not subject to the largest slope errors located off center. The ray tracing results show that most of the thermal induced focus blurring at the SSA occurs between 5-7 keV. By having the HFM bendable the focal distance can be adjusted to partly compensate for the thermal dent on the crystal.

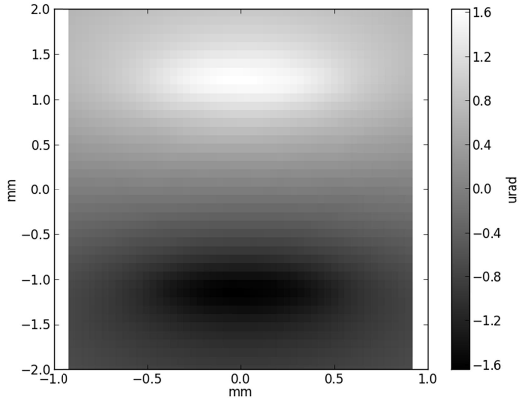

Figure 5. Slope errors on the first crystal in the monochromator at 5000 eV. Slope error in meridional direction (left) and sagittal direction (right). Photon beam direction is upwards.

3.2. Ray tracing results

Figure 6 shows intensity distributions on the secondary source aperture for two photon energies, 5000 eV and 8333 eV. The spot size is largest for 5000 eV due to the heat induced slope error on the first monochromator crystal. Already for the photon energy 8333 eV the spot size is considerably smaller and similar to what is seen for higher energies. To guide the eye a 20x20 μm^2 aperture is indicated as a rectangle in the images. Table 4 shows full-width half-maximum (FWHM) values for different photon energies.

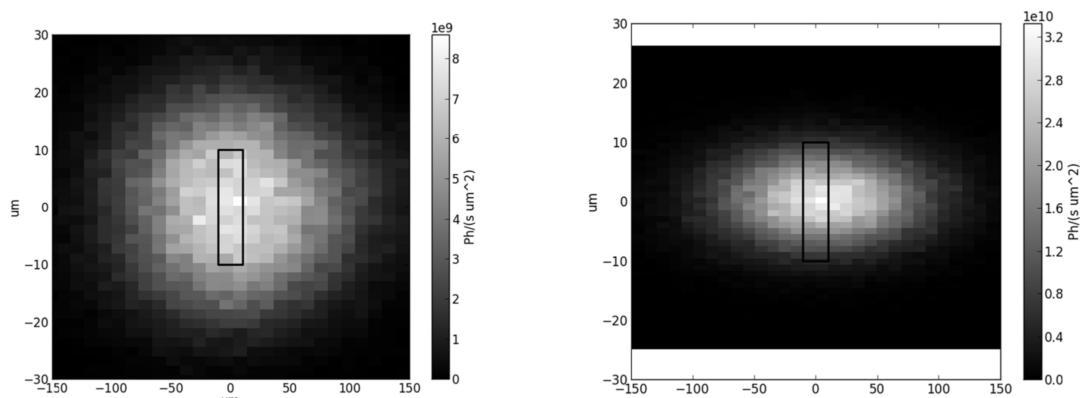

Figure 6. Irradiance on the secondary source aperture for 5000 eV (left) and 8333 eV (right). The rectangle indicates the size of a 20x20 μm^2 aperture.

We expect to see somewhat larger spot sizes on the SSA, especially for the higher energies, because mirror surface roughness will enlarge the spot. The indicated aperture size is not optimal in the vertical direction. If the aperture size is of the same size as the spot, height vibrations in the beam will translate into intensity fluctuations at the experimental stations. By using an aperture substantially smaller than the spot size the beam passing the aperture will consist of the core part and thus result in stable beam intensity.

After the secondary source aperture the beam is divergent. The zone plate position is 33 meters from the secondary source aperture and the KB position 43 meters. The illumination at these two positions, for 5.0 and 25 keV, is shown in figure 7. The circle indicates a 300 µm diameter. We find that the illumination extends over the whole nano focusing optics but does not overfill extensively which is important to avoid losing valuable intensity in the final spot on the sample.

Table 4. Spot sizes on the secondary source aperture. The aberration free geometric spot size is calculated from the undulator source size and the optics entrance and exit arms.

Photon energy (eV)	Horizontal size FWHM (μm)	Vertical size FWHM (μm)
5000	124	30
8333	115	13
11667	125	13
25000	120	10
Geometric image	112	9.6

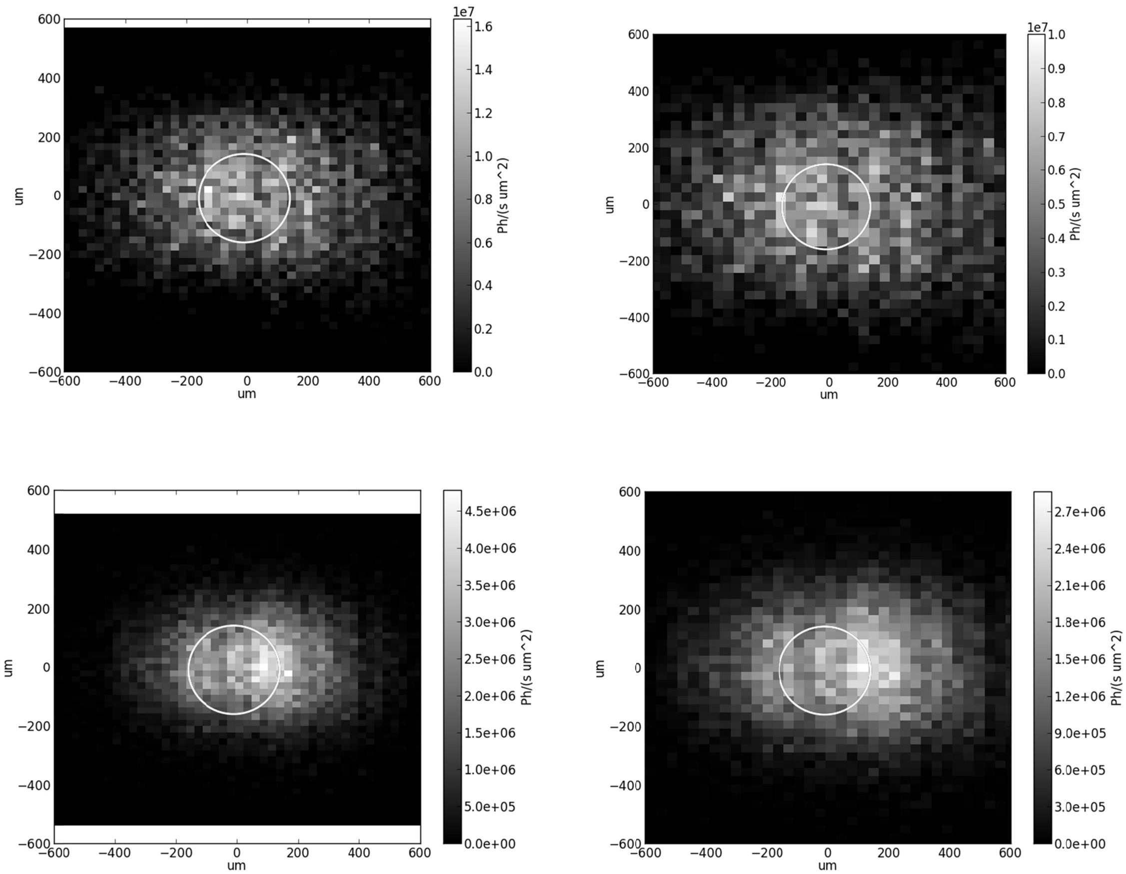

Figure 7. Irradiance at the nano-focusing optics positions. Left column: Zone plate position at 33 meter from the SSA. Right column: KB-optics position at 43 meter from the SSA. Top row: 5000 eV, bottom row: 25000 eV. The white circles are 300 μm in diameter and correspond to the largest foreseeable zone plate or the approximate acceptance area of the KB-optics.

Photon fluxes incident on the secondary source aperture, after the aperture, and at the FZP and KB-optics positions have been simulated, see figure 8. The results have been calculated with ray tracing simulations in MASH, taking into account undulator properties, mirror reflectivity, monochromator transmission, losses due to power load deformations, polarization etc.

The curves in figure 8 are calculated with a SSA opening of 20 x 20 μm^2. In order to reach the diffraction-limited spot size of the zone plate it has to be illuminated coherently. By adjusting the SSA opening the coherence length[13] can be adapted to the diameter of the zone plate and to the photon energy. As an example, with a zone plate diameter of 150 μm operating at 10 keV and 33 meter distance, the SSA opening should be set to 12 μm. The photon flux incident on the zone plate is, with these parameters, estimated to 1×10^{12} photons/s. If we assume the zone plate efficiency to be a few percent, the flux at the sample will be in the 10^{10} photons/s range at 10 keV.

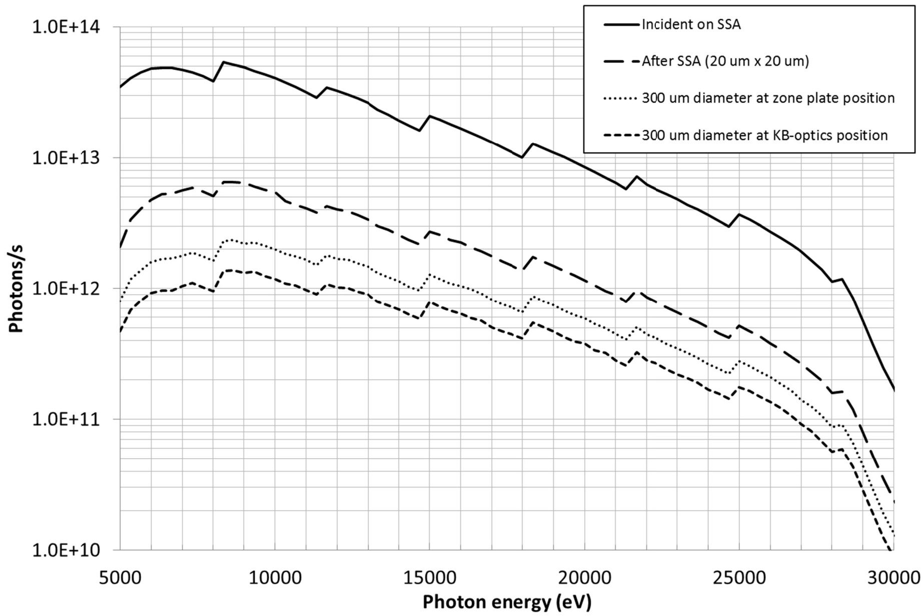

Figure 8. Photon flux incident on the secondary source aperture, after the aperture, and at the FZP and KB-optics positions. The steps in the curves occur when changing undulator harmonic along the photon energy axis. The three lower curves are based on an SSA opening of 20 x 20 μm^2.

4. SUMMARY

The NanoMAX beamline will be a very competitive and versatile hard X-ray imaging beamline aiming for a 10 nm spatial resolution with high photon flux taking advantage of the extraordinary low emittance of the MAX IV 3 GeV storage ring. The beamline will have two experimental stations allowing for different sample setups and detection modes. The commissioning phase will start early 2016 and by the end of 2016 we plan to be in operation.

ACKNOWLEDGEMENT

We would like to thank colleagues for valuable comments to the optical design work. Especially we are grateful for recommendations from the panel with experts from APS, ESRF and Petra III that has reviewed the optical design. The NanoMAX beamline is funded by the Knut and Alice Wallenberg foundation together with twelve Swedish universities.

REFERENCES

[1] Ice, G. E., Budai, J. D. and Pang, J. W. L., "The Race to X-ray Microbeam and Nanobeam Science," Science 334(6060), 1234-1239 (2011).

[2] Somogyi, A., Kewish, C. M., Polack, F. and Moreno, T., "The Scanning Nanoprobe Beamline Nanoscopium at Synchrotron Soleil," AIP Conf. Proc. 1365, 57-60 (2011)

[3] Schroer, C. G., Boye, P., Feldkamp, J. M., Patommel, J., Samberg, D., Schropp, A., Schwab, A., Stephan, S., Falkenberg, G., Wellenreuther, G. and Reimers, N., "Hard X-ray nanoprobe at beamline P06 at PETRA III," Nucl. Instr. Meth. In Phys. Res. A616, 93-97(2010).

[4] Martínez-Criado, G., Tucoulou, R., Cloetens, P., Bleuet, P., Bohic, S., Cauzid, J., Kieffer, I., Kosior, E., Labouré, S., Petitgirard, S., Rack, A., Sans, J. A., Segura-Ruiz, J., Suhonen, H., Susini, J. and Villanova, J., "Status of the hard X-ray microprobe beamline ID22 of the European Synchrotron Radiation Facility," J. Synchrotron Rad. 19, 10-18 (2012).

[5] Winarski, R. P., Holt, M. V., Rose, V., Fuesz, P., Carbaugh, D., Benson, C., Shu, D. M., Kline, D., Stephenson, G. B., McNulty, I. and Maser, J., "A hard X-ray nanoprobe beamline for nanoscale microscopy," J. Synchrotron Rad. 19, 1056-1060 (2012).
[6] Tanaka, T. and Kitamura, H. "SPECTRA: a synchrotron radiation calculation code," J. Synchrotron Rad. 8, 1221-1228 (2001).
[7] [SPECTRA, http://radiant.harima.riken.go.jp/spectra/index.html].
[8] Song, Y., Hormes, J, and Kumar, C. S. S. R., "Microfluidic Synthesis of Nanomaterials," Small 4(6), 698–711 (2008).
[9] Andersen, T., Jensen, R., Christensen, M. K., Pedersen, T., Hansen, O. and Chorkendorff, I., "High mass resolution time of flight mass spectrometer for measuring products in heterogeneous catalysis in highly sensitive microreactors," Rev. Sci. Instrum. 83(075105), 1-5 (2012).
[10] Sondhauss, P., [X-ray Optics for the Short Pulse Facility, MAX-lab internal report January], MAX IV Laboratory, (2011).
[11] Lai, B. and Cerrina, F.,"Shadow – a synchrotron radiation ray tracing program," Nucl. Instr. Meth. In Phys. Res. A246, 337-341 (1986).
[12] [COMSOL Multiphysics, http://www.comsol.se/products/multiphysics].
[13] Attwood, D., [Soft X-rays and extreme ultraviolet radiation], Cambridge University Press, Cambridge United Kingdom, 300-306 (1999).